ScienceDirect®

Multimodal plant recognition through hybrid feature fusion technique using imaging and non-imaging hyper-spectral data

Pradip Salve [a] 👤 ✉ , Pravin Yannawar [a], Milind Sardesai [b]

Show more ⌄

:≡ Outline | ⛓ Share 💬 Cite

Referred to by   **Erratum regarding missing Declaration of Competing Interest statements in previously published articles**

Journal of King Saud University - Computer and Information Sciences, Volume 32, Issue 10, December 2020, Pages 1216

📄 View PDF

Abstract

Automatic classification of the plants is growing area of association with computer science and Botany, it has attracted many researchers to subsidize plant classification using image processing and machine learning techniques. Plants can be classified using number of traits such as leaf color, flowers, leaves, roots, leaf shape, leaf size etc. highly depends upon feature selection methods. However extraction of features from selected trait is most significant state in classification. State-of-the-art classification can be achieved by using leaf characteristics such as leaf venation patterns, leaf spectral signatures, leaf color, leaf shape, etc. This paper describes multimodal plant classification system using leaf venation patterns and its spectral signatures as a significant features. This paper shows that the feature fusion can be used to achieve efficient plant identification. The accuracy of identification for leaf spectral data, leaf venation features and HOG features is validated, it signifies that feature fusion technique performs better than that of non-

imaging spectral signatures features only, with recognition result of 98.03% GAR and 93.51% GAR, respectively.

Questions answered in this article

- ∨ What features were used for multimodal plant identification?

- ∨ What is the purpose of the multimodal plant identification system?

- ∨ What is the relationship between leaf venation and leaf spectral signatures?

- ∨ What is the importance of leaf analysis in plant taxonomy?

- ∨ What was the accuracy achieved using feature level fusion?

< Previous   Next >

Keywords

1. Introduction

Leaf analysis has very important and extensively used area in the field of plant taxonomy to understand, recognize and analyze leaf patterns and plant recognition. The Automatic plant retrieval based on leaf have been widely explored, based on leaf shape, color, leaf texture and other geometric features have been used widely (Green et al., 2014, Salve et al., 2016). Recently the most significantly studied feature is shape, venation and spectral signature indices of the leaf, also referred to as main feature due to its homogeneity in venation patterns as well as spectral signature patterns. Leaf venation patterns possesses leaves characteristics with a specific structure, which may be useful to identify plant species. The important factor is to effectively extract the leaf structure and acquire leaf spectral signatures; with regard to, few techniques have been proposed to efficiently extract leaf vein structure. However, there have been few efforts to evaluate and correlate leaf venation and leaf spectral signatures; furthermore, numerous methods exploited manually or semi-automatic leaf venation extraction from leaf samples.

Leaf vascular bundles are correlated with the taxonomic groups of plants and with the shapes of leaves. Which possesses characteristics like length of primary veins, number of secondary veins, its area, perimeter, convex hull etc. Along with geometric features it also provides visual textual

information, color information, pores on the leaves but among all the characteristics veins are consider to be more significant due to its uniqueness. Varying in the density of the network and the distance between the larger veins. In addition, the number of loops in the pattern can also help determine the leaf species.

1.1. Related work

Various approaches have been implemented in order to achieve state-of-the-art plant identification. We have studied and categorize the plant classification approaches based on feature selection techniques. This section provides the review of most commonly used methods based on venation, geometric + morphological and spectral data based approaches adopted by many authors.

1.2. Venation based

Norbert Kirchgeßner et al. (2002) have proposed a technique for robust extraction of leaf veins on plant leaf samples. Authors have proposed and utilized structure tracking by taking leaf image spatial information. The b-spline have been adopted to show the resultant leaf venation patterns as its contains the hierarchical information of leaf vein system. Experiments have been carried on short images with 480*640 pixels. To measure the direction of veins quality measure of first and second order have been adopted. The stopping criteria for vein search is marked by masks which indicates the region where the veins found.

Ḿonica G. Larese et al. (2014) classified legume leaf images of soybean, white bean and red bean plants, proposed an algorithm able to considering only the leaf vascular patterns. Other geometric and visual characteristics have been excluded. Leaf images have been captured with a standard scanner and vein segmentation has been achieved by using the Unconstrained Hit-or-Miss Transform (UHMT) with the help of adaptive thresholding. They have measured many morphological features on the vascular network and classify those using Random forests. Many morphological features have been. Many other venation traits have been measured on the segmented leaf, further classification have been done by using four different classifiers random forests, penalized discriminant analysis, support vector machines using both linear and Gaussian kernels.

To extract leaf veins a new approach that combines an artificial neural network (ANN) classifier and a thresholding method is proposed by H. Fu et al. (Fu and Chi, 2006). Firstly carried out to coarsely determined vein regions then intensity histogram has been used firstly for the leaf image segmentation. Trained ANN classifier has been used for the segmentation purpose and used each object pixels used as a inputs, then features have been extracted using a window centered on the pixels. H. Fu et al. have compared with other methods and concluded, the combined approach is capable of extracting more accurate venation modality of the leaf for the subsequent vein pattern classification.

Firstly by analyzing leaf venation, JinKyu Park et al. (2008) and used for leaf categorization. Then

found similar leaves using extracted and utilized leaf shape features from the already classified group of leaf dataset. Authors have used the same approach as blood vessels extraction. Jin Kyu Park et al. have proposed scope corner detection method.

Density of the feature points have been measures using a non-parametric estimation of the density then selected points have been categorized. Lastly concluded that the proposed techniques effectiveness by performing several experiments on a prototype system.

Anne-Gaëlle Rolland-Lagan et al. (2009) have used rosette leaf of Arabidopsis thaliana to quantify leaf venation patterns throughout a series of developmental stages of the plant. Characterized the shape and size of venation patterns and its areoles (loops), which increases and get twisted while the growth of the leaf. Also observed a distal to proximal gradient of loop shape its length or width ratio which varies over time and margin-to-center gradient in loop sizes. it observed that there is two-link amongst theoretical models of leaf shape patterning and molecular experimental work to study the vascular patterning while development of the leaf.

Xiaodong Tang et al. (2009) proposed a leaf vein extraction algorithm to extract the sample leaf from the images with complicated background. The marker-controlled watershed segmentation technique has been adopted and the three channels of HSI color space have been separated and produced the gradient images individually. The solidity (integrity) measure have been utilized to estimate the segmented images for extraction of the sample leaf and verified the final leaf extraction results.

James S Cope et al. (2010) Genetic algorithms have been utilized to regress a set of classifiers to find the leaf veins. the proposed technique is able to extract the vascular structure from leaf sample. The analysis of the produced classifier have been performed by qualitatively and quantitatively. The neighborhood around the current pixel was measured by 11*11 size window to compute the local gradient direction of pixels. Further those pixels considered as vein points. The proposed method is able to achieve primary and secondary venation patterns with having slight noise around it. Finally results were also compared to ant colony algorithm.

Joanna Sekulska-Nalewajko et al. (2010) The quantitative analysis approach have been adopted to segment the leaf venation. The leaf background colour have been utilized to differentiate the foreground leaf as a target object in various colour space. The hue or saturation channel have been used to segment the leaf blade by thresholding HSV color space or by thresholding luminance image.

Jinane Mounsef et al. (Mounsef and Karam, 2011) have proposed a technique to extract the spatial leaf venation patterns from leaf images automatically. Leaf vein density vein reticulation (loops) sizes and shapes have been utilized as a features (Price et al., 2011). The experiments have been carried out on leaf of Arabidopsis thaliana while leaf have been developing. The size and shape of the leaf network reticulation which increases and get twisted by new vein as a leaves develops, have been characterized by skeletonization and other imaging techniques. The approach enables

interactive way to the users to batch process a throughput of data.

Price, Charles A., et al. (2011) have been developed the Leaf Extraction and Analysis Framework Graphical User Interface (LEAF GUI), semi-automatic software tool that allow users to study the improved empirical understanding of leaf network structure. It takes a leaf image as an input and enhances leaf veins relative to the background. then follows the consequent steps of the interactive thresholding and cleaning steps, it returns the qualitative and quantitative analysis results of leaf vascular structure and venation loops. The statistics measure includes the dimensions of the network, position and connectivity of all network vein, of the areoles they surrounded by.

1.3. Leaf characteristics based approach

Snehal Shejwal et al. (2015) have developed Smartphone application which is used for plant classification. Probabilistic Neural Network (PNN), Support Vector Machine and Fuzzy logic, k-nearest neighbor (k-NN) classifier have been adopted for classification purpose. Open Source Database SQLite was used and embedded in Android device.

Nursuriati Jamil et al. (2015) have proposed low level features for inter and intra-class plant identification, 455 leaves of herbal medicine has used to carry out the experiments. The dataset is divided into 70% & 30% ratio for training and testing respectively. Scale Invariant Feature Transform (SIFT) was used to extract shape features, color moments used for color features, and Segmentation-Based Fractal Texture Analysis (SFTA) for texture features (Wang et al., 2014). Results demonstrate that single texture feature outperformed colour, or shape feature achieving 92% accuracy. While, fusion of three features (SIFT + SAFTA + color) got 94% recognition rate.

A. C. Siravenha et al. (Siravenha and Carvalho, 2016) was adopted leaf textures features by combining a multi-resolution technique, Discrete Wavelet Transform (2D-DWT), statistical models and Gray-Level Co-occurrence Matrices (GLCM), were used to perform classification. Flavia database have been used to carry out the experiments. An overall classification accuracy was achieved 91.85%.

1.4. Leaf spectral signature based

Yachao Wang et al. (Wang et al., 2014) have used five different types of discriminant analysis classifiers viz. Linear, Quadratic, DiagLinear, Diag Quatic and Mahalanobis, with data reduction based on principal components analysis (PCA) and independent component analysis (ICA). Proposed classification model achieved accuracy is about 98.35% with dimension 25 reduced from 2500.

A. B. Varpe et al. (2015) proposed plant species recognition system based on non-imaging hyperspectral data and designed own database for experiment. The overall accuracy 91% was achieved through SVM.

2. Methodology

We have done various experiments to achieve and validate plant identification system. For identification and verification we have used System based verification using FAR, FRR, ERR and GAR generally used in biometric systems. The proposed work mainly focused on leaf venation patterns and leaf spectral signatures i.e. non-imaging features, leaf images from *VISLeaf* dataset used throughout the experimental work. The dataset was organized with 60 plant species collected from the Botanical garden of Dr. Babasaheb Ambedkar Marathwada University campus, Aurangabad (MS) India. Each species includes 10 scanned images and 10 hyper spectral signature data for 60 plant species listed below. Therefore there are totally 600(60*10) images in the proposed dataset. Fresh leaf samples were taken from Botanical Garden during data collection and scanned with the resolution of 300 dpi. Scientific nomenclature related to the sample was also verified from taxonomical experts. Subsequently these scanned samples were pre-processed and voted for feature extraction. The extracted features were saved on the machine as training set template and later used against testing test for recognition purpose. The Spectral signatures were acquired using the ASD Field Spec 4 Spectro-radiometer instrument. 350–2500 nm wavelength of the ASD instrument was set during acquisition processes which is same as hyper spectral non-imaging data. The spectral resolution was set to be 3 nm to 2500 nm with sampling interval 2 nm. White reference panel was used for optimization and calibration of device to achieve absolute reflectance in lab conditions before samples recording. Spectral data obtained under artificial light sources. Halogen lamp with 75w delivered with the ASD device used for artificial light sources. It was used to record the plant samples by zenith angle of 600 from the distance of 45 cm above the samples. The field of view (FOV) was 8 degree and fiber-optic cable was set as of off-nadir position. 10 leaf samples from each plant were recorded for receiving spectra. The RS3 (Version 6.3) software was used for recording the reflectance spectra of leaves. Fig. 1 shows spectral data collection using ASD instrument. ASD instrument produced "*.asd*" file extension data format containing of reflectance and wavelength of spectra. The file was imported in MATLAB software and used reflectance of the spectra in the experiments (See Fig. 2).
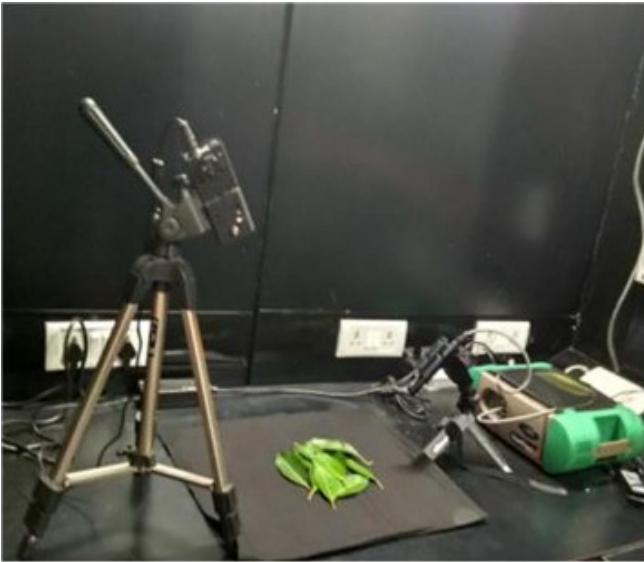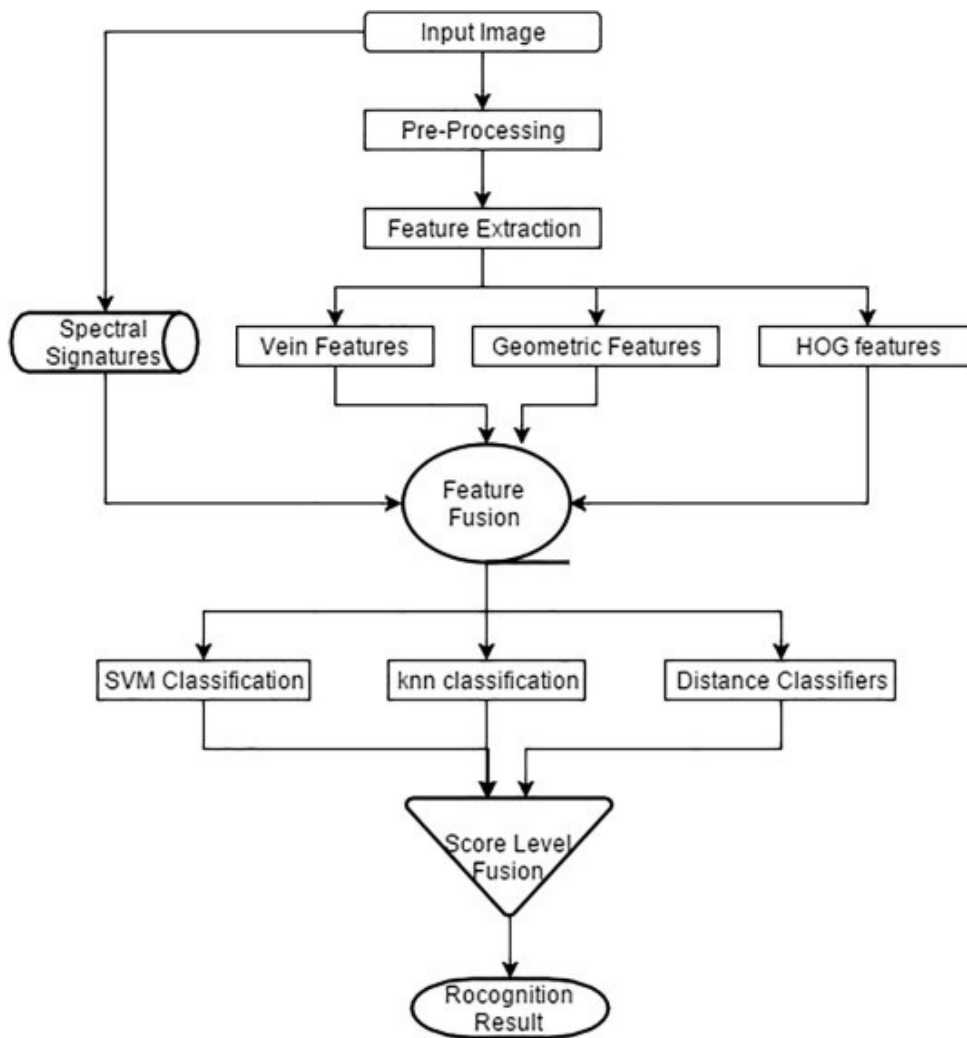
Download : Download high-res image (81KB)

Download : Download full-size image

Fig. 1. ASD instrument with sample.

Fig. 2. Flow diagram.

2.1. List of Plant with Scientific name used in our experimental work

Acalypha indica L, Aegle marmelos (L.) Corrêa, Anacardium occidentale L, Antigonon leptopus Hook. Arn., Argemone mexicana L, Azadirachta indica A.Juss, Barleria prionitis L, Bauhinia racemosa Lam, Boerhavia diffusa L, Bougainvillea spectabilis Willd, Butea monosperma (Lam.) Taub, Caesalpinia bonduc (L.) Roxb, Calotropis procera (Aiton) Dryand, Cassia siamea Lam, Cinnamomum verum J.Presl, Cissus repanda Vahl, Cissus repens Lam, Citrus aurantiifolia (Christm.) Swingle, Coccinia grandis (L.) Voigt, Cocculus hirsutus (L) W Theob, Corchorus olitorius L, Euphorbia geniculata Ortega, Euphorbia hirta L, Ficus benghalensis L, Ficus virens Aiton, Gliricidia sepium (Jacq.) Walp, Grewia hirsuta Vahl, Hamelia patens Jacq, Hibiscus rosa-sinensis L, Hiptage benghalensis (L.) Kurz, Holoptelea integrifolia Planch, Ipomoea nil (L.) Roth, Ipomoea pes-tigridis L, Jasminum nudiflorum Lindl, Jatropha integerrima Jacq, Kigelia africana (Lam.) Benth, Lantana camara L, Leonotis nepetifolia (L.) R.Br, Mangifera indica L, Mimusops elengi L, Morinda pubescens Sm, Nerium oleander L, Parthenium hysterophorus L, Peristrophe

bicalyculata (Retz.) Nees, Pithecellobium dulce (Roxb.) Benth, Plectranthus mollis (Aiton) Spreng, Polyalthia longifolia (Sonn.) Thwaites, Punica granatum L, Senna tora (L.) Roxb, Spathodea campanulata P.Beauv, Syzygium cumini (L.) Skeels, Tamarindus indica L, Tecoma stans (L.) Juss. ex Kunth, Tephrosia villosa (L.) Pers, Terminalia bellirica (Gaertn.) Roxb, Tinospora sinensis (Lour.) Merr, Trigonella foenum-graecum L, Ventilago maderaspatana Gaertn, Withania somnifera (L.) Dunal, Ziziphus jujuba Mill.

2.2. Feature extraction

The multimodal plant identification system accepts the non-imaging leaf spectral signatures as a features and visual features viz. Leaf Venation features such as number of veins present in the leaf, length of each vein, orientation of each vein, Histogram of Gradients (HOG) features and geometric features.

2.3. Extraction of spectral signatures

We have acquired spectra of each plant leaf sample using ASD field spect4 instrument. The process of data collection shown in Fig. 1. ASD Feildspect 4 instrument produces "*.asd*" file extension by using inbuilt software RS3 (Version 6.3). Furthermore we have imported this file to MATLAB software for extracting a reflectance and wavelength of the sample. In this piece of work we have used only reflectance as a feature. Each sample produced a 1*2100 dimension feature matrix. For the time and space efficiency we reduced a size of data to 1*500 size. Fig. 3 shows the sample plot of *Ipomoea nil (L.) Roth, Pithecellobium dulce* (Roxb.) Benth. plant. Table 1. Shows the actual features and dimension of data extracted from spectral signature (See Fig. 4).
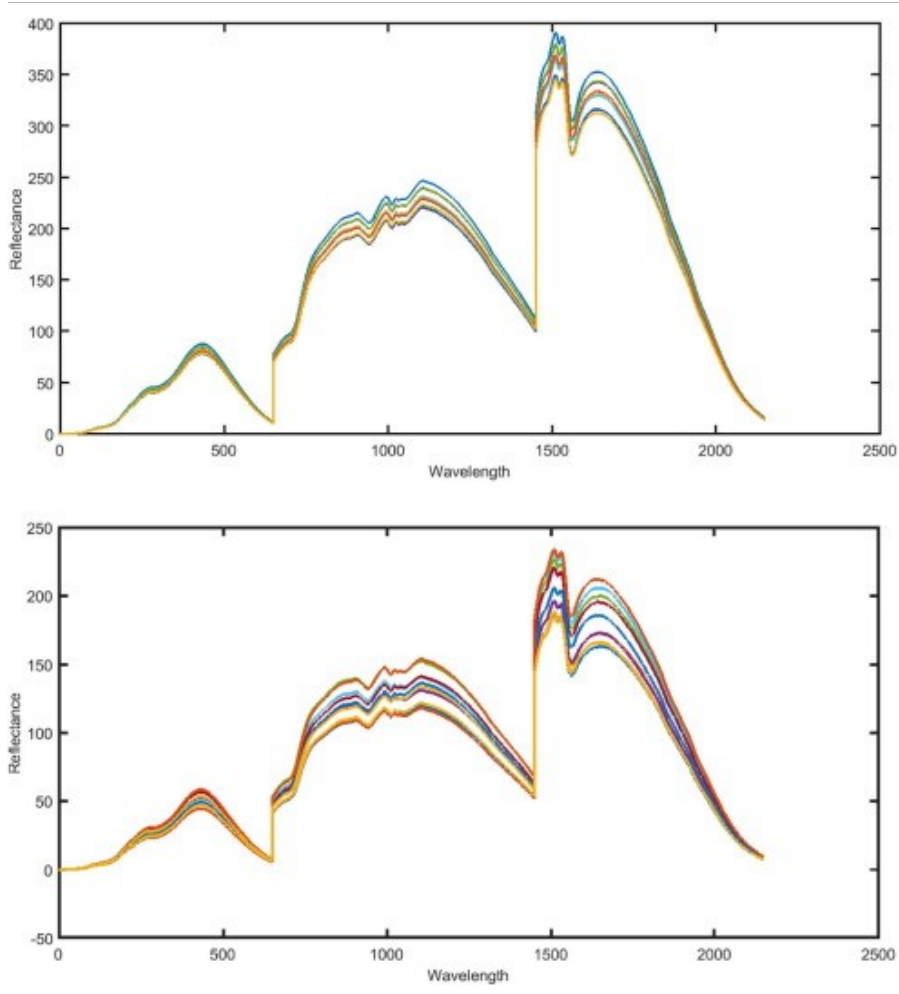
Fig. 3. Spectral Signatures plot of plant *Ipomoea nil (L.) Roth, Pithecellobium dulce (Roxb.) Benth.,* respectively, plotted using Matlab.

Table 1. Sample of Feature Matrix after extraction of spectral signatures of plant *Cocculus hirsutus (L.) W. Theob* 10 samples per each plant.

	1	2	3	4	5	6	7	8	9	10	n	500
Sample 1	0.47	0.498	0.543	0.589	0.621	0.659	0.695	0.73	0.779	0.843	:	36.703
Sample 2	0.455	0.472	0.51	0.566	0.624	0.645	0.66	0.703	0.771	0.844	:	37.611
Sample 3	0.441	0.497	0.525	0.527	0.599	0.631	0.645	0.677	0.74	0.817	:	36.638
Sample 4	0.459	0.493	0.506	0.514	0.581	0.625	0.653	0.687	0.736	0.807	:	36.836
Sample 5	0.492	0.506	0.548	0.603	0.627	0.667	0.705	0.735	0.815	0.869	:	27.339
Sample 6	0.502	0.492	0.513	0.57	0.638	0.712	0.749	0.752	0.835	0.902	:	26.941

	1	2	3	4	5	6	7	8	9	10	n	500
Sample 7	0.44	0.493	0.551	0.586	0.633	0.658	0.692	0.748	0.779	0.84	:	27.515
Sample 8	0.463	0.496	0.537	0.576	0.606	0.654	0.685	0.692	0.76	0.856	:	27.618
Sample 9	0.456	0.511	0.562	0.592	0.657	0.679	0.704	0.762	0.797	0.844	:	27.116
Sample 10	0.294	0.302	0.315	0.335	0.357	0.408	0.412	0.359	0.445	0.469	:	7.888
:	:	:	:	:	:	:	:	:	:	:	:	:
Sample 420th	:	:	:	:	:	:	:	:	:	:	:	:
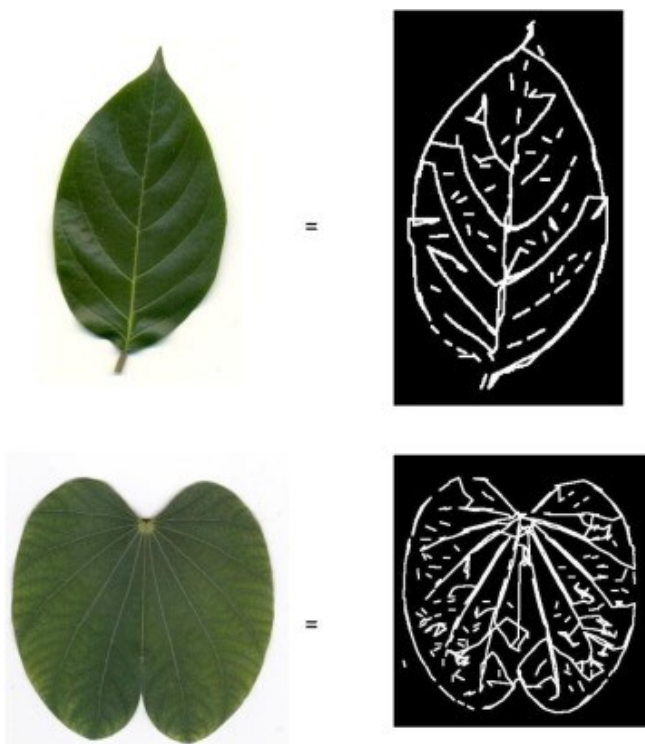
Download : Download high-res image (151KB)

Download : Download full-size image

Fig. 4. Sample leaf venation produced from original images.

2.4. Extraction of venation features

The color image is composed of three channels i.e. (R + G + B) Firstly from the input color image, we have selected green channel due to the color dominancy of green in the leaf image. Further we converted G channel image to Discrete Wavelet Transform for the noise removal and better conservation of edge because the edge is the most significant information of a digital image towards the extraction of better leaf venation pattern. The traditional filter make the image blurry and reduce the information from image. So we have to preserve the edge of the leaf sample while

reducing the noise of the image. So we have implemented Discrete wavelet transform method to reduce noise and protect the edges.

$$\psi(x) = \sum_{k=-\infty}^{\infty} (-1)^k a_{N-1-k} \psi(2x - k) \tag{1}$$

where N is an even integer. Note that usually only few of the coefficients a, k are nonzero which simplifies the calculations. After binarization we able to produce leaf venation patterns image.

The venation angle of each vein is calculated by the formula:

$$\theta = tan^{-1}\left(\frac{Gy}{Gx}\right) \tag{2}$$

2.5. Histogram of oriented gradients (HOG)

The HOG descriptors are local statistic of the orientations of the image gradients around key points (Xiao et al., 2010, Dalal and Triggs, 2005). The leaf sample was divided into M*M cells after preprocessing; each of the cell has a pixel size of $N*N$. By using the Eqs. (1) and (2) we have computed gradient magnitude g and the gradient orientation θ were for all the pixels in the block; the derivatives (g_x) and (g_y) of the image I were computed with pixel differences using Eqs. (3) and (4).

$$g(\phi, \omega) = \sqrt{g_x(\phi, \omega)^2 + g_y(\phi, \omega)^2} \tag{3}$$

$$\theta(\phi, \omega) = \arctan \frac{g_y(\phi, \omega)^2}{g_x(\phi, \omega)^2} \tag{4}$$

$$g_x(\phi, \omega) = I(\phi + 1, \omega) - I(\phi - 1, \omega) \tag{5}$$

$$g_y(\phi, \omega) = I(\phi, \omega + 1) - (\phi, \omega - 1) \tag{6}$$

After gradient computation, each pixel within a cell casts a weighted vote for an orientation-based histogram based on the gradient magnitude and orientation. This histogram divides the gradient angle range into K bins. Then we normalized all cells' the histograms in block to reduce the effect of noise and overlapping of cells. We consider the histogram in the same cell as a feature. Let F be the feature, and for getting feature vector we used the function is as follows:

$$F = \frac{F}{\sqrt{\|F\|_2^2 + \epsilon^2}} \tag{7}$$

The histograms of all the blocks combined into a whole HOG descriptor. For example, the HOG feature extraction work, we set the Block size of 3 × 3 cells, and the number of bins, K, is set to 9. As a result, algorithm calculates 81(3*3*9) blocks, so the dimension of overall HOG feature is 81 for each image.

Finally we produced 1*81 dimension feature vector from HOG descriptor and fused it to Spectral

features, vein features and geometric features. Table 2 shows the sample matrix of all fused features.

Table 2. Sample of fused Feature Matrix of spectral signatures + vein features + geometric + HOG descriptor features for the plant "*Cocculus hirsutus (L.) W. Theob*" 10 samples per each plant.

	1	2	3	4	5	6	7	8	9	10	n	620
Sample 1	0.228	0.227	0.232	0.392	0.336	0.241	0.241	0.228	0.238	0.388	:	0.392
Sample 2	0.185	0.162	0.208	0.492	0.291	0.219	0.183	0.163	0.199	0.539	:	0.327
Sample 3	0.205	0.209	0.235	0.476	0.252	0.219	0.204	0.2	0.239	0.521	:	0.28
Sample 4	0.231	0.211	0.241	0.469	0.249	0.22	0.237	0.212	0.236	0.498	:	0.281
Sample 5	0.132	0.116	0.138	0.592	0.24	0.12	0.134	0.114	0.134	0.629	:	0.268
Sample 6	0.175	0.18	0.176	0.389	0.43	0.164	0.182	0.195	0.176	0.357	:	0.543
Sample 7	0.166	0.17	0.178	0.489	0.326	0.178	0.185	0.145	0.171	0.548	:	0.36
Sample 8	0.154	0.135	0.15	0.481	0.385	0.156	0.156	0.137	0.144	0.512	:	0.436
Sample 9	0.146	0.141	0.151	0.519	0.335	0.145	0.159	0.129	0.144	0.563	:	0.374
Sample 10	0.265	0.273	0.282	0.347	0.282	0.263	0.27	0.268	0.295	0.357	:	0.309
n	:	:	:	:	:	:	:	:	:	:	:	:
Sample 180th	:	:	:	:	:	:	:	:	:	:	:	:

1 to 500 Spectral features   501 to 620 fused vein features

2.6. Feature normalization

The calculated features saved in system for further experiments. The saved feature matrix then normalized to reduce variance in features. The normalization of features were carried out using the Eq. (8)

$$NF = \frac{FV - \mu}{\sigma} \tag{8}$$

where *FV* is the feature vector and μ is mean of feature vector and σ standard deviation.

2.7. Identification technique

In this section the feature vectors from each feature extraction technique was received to perform the classification. The feature vectors was divided in to training set and testing set by 70%, 30% respectively. The size of training set was 420 samples and 180 samples for testing from different plant classes. To obtain the score matrix the Euclidean distance measure was used and calculated by the Eq. (9)

$$S(i,j) = \sqrt{\sum_{i=1}^{n} (q_i - p_j)^2} \tag{9}$$

The score matrix was generated and passed to decision making which determine which class belong to. To generate the threshold value for each leaf sample we have driven the steps to generate threshold value from (Wu et al., 2007) which can summarize as the following:

$$\Delta = \frac{\max(FV_i) - \min(FV_j)}{\beta} \tag{10}$$

where β is a constant pre-determined which is used to divide threshold value into N parts.

$$\theta i = \min(FV) + \Delta i \tag{11}$$

$\theta i (i = 1, 2,\ldots,N)$ is selected when the value approaches the FRR or FAR value is very small depending on the specifications required.

2.8. Decision criteria

Finally the decision has been made from Threshold value *(T)*. System accepts the identity of the leaf sample *(if DS ≤ T)* or rejects **(???? D??>??)**. Where DS is the distance score between samples.

2.9. Evaluation criteria

The evaluation has been carried out using False acceptance rate (FAR), False rejection Rate (FRR) and the Equal error rate (EER), Genuine Acceptance Rate (GAR).

False Acceptance Rate (FAR) is the percentage of unknown samples accepted by identification system. FAR can be calculated using Eq. (12)

$$FAR = \frac{the\ score\ of\ inter\ class\ samples(Impostor) >\ threshold}{number\ of\ all\ impostor\ score}\ X\ 100 \tag{12}$$

FRR is the percentage of known samples rejected by the identification system. The FRR was calculated using Eq. (13)

$$FRR = \frac{score\ of\ inter\ class\ samples(Genuine) < threshold}{number\ of\ all\ genuine\ score}\ X\ 100 \tag{13}$$

ERR is the intersection point plotted on the graph where FAR and GAR intersects each other. The EER is try to measure the FAR performance against another FRR (The lowest the ERR the highest the accuracy) by finding the equal (the nearest to equal or have the min distance in case if not equal) between False Acceptance Rate (FAR) and False Rejected Rate. ERR can be calculated using Eq. (14)

$$ERR = \frac{FAR + FRR}{2} \tag{14}$$

2.10. Genuine Acceptance Rate (GAR)

This is defined as a percentage of genuine leaf samples accepted by the system. GAR have been calculated using Eq. (15):

$$GAR = 100 - FRR \tag{15}$$

3. Experimental results

The identification of plants was produced using leaf spectral signatures non-imaging data and scanned leaf samples. The spectral signature features were collected from 60 plant species each plant 10 leaf samples and stored on disk for classification purpose. Similarly 60 plant species were used for imaging data i.e. scanned photos of plant leaves 10 per species. The experimental work has been carried out on five type of features namely Vein Features, HOG Features, Geometric features proposed in (Ali et al., 2017), Spectral Sign. Features, All features fused together.

3.1. Vein pattern feature based recognition

The score (S) and threshold (T) has been produced to evaluate the plant identification by using vein features. The score matrix generated through "Euclidean distance measure" have been divided into Genuine (Intra class samples) score and Impostor score (Inter class samples) based upon the threshold value while (S ≤ T) yields Genuine and (S > T) yields Impostor scores. Further the genuine and impostor used to calculate FAR and FRR. Fig. 5 shows the relation between FAR and FRR based on threshold value. It is observed that the efficient system was achieved when ERR equal to 21.48% and FAR, FRR equal to 20.30%, 22.66% respectively. Table 3 shows the maximum GAR is achieved 78.51% with 0.13 threshold. Fig. 6 shows the ROC curve with relation to the FAR against GAR.
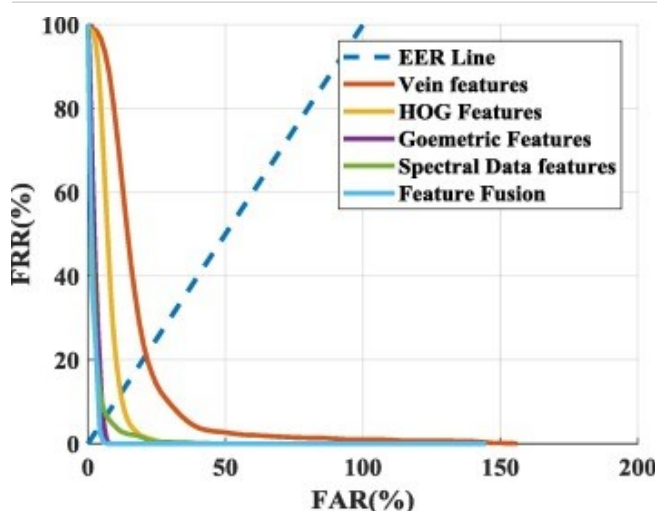
Download : Download high-res image (160KB)
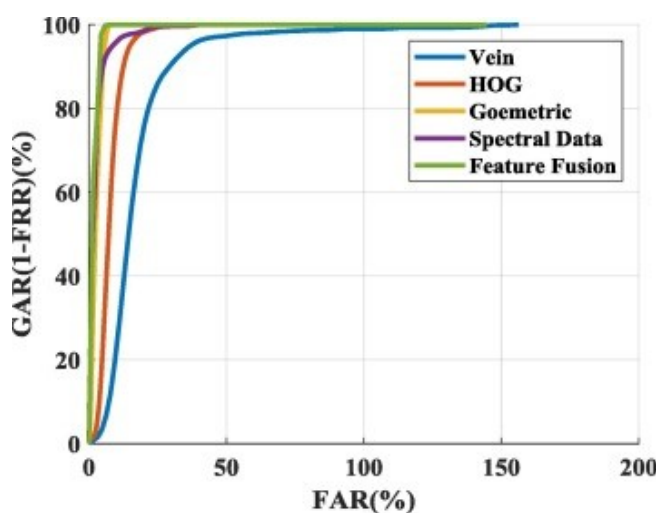
Download : Download full-size image

Fig. 5. The performance of all features plotted within single graph shows relation of FAR vs. FRR based on threshold value.

Table 3. Performance of the system based on **Vein Features** method on optimal threshold values.

Threshold	FAR (%)	FRR (%)	EER (%)	GAR (%)
0.1	15.61741	42.06667	28.84204	71.15796
0.13	**20.30264**	**22.66667**	**21.48465**	**78.51535**

	Threshold	FAR (%)	FRR (%)	EER (%)	GAR (%)
Vein features	0.2	31.23483	8.733333	19.98408	80.01592
	0.3	46.85224	2.933333	24.89279	75.10721
	0.4	62.46966	2	32.23483	67.76517
	0.5	78.08707	1.4	39.74354	60.25646

Download : Download high-res image (133KB)

Download : Download full-size image

Fig. 6. ROC curve of FAR vs. GAR of all features plotted within single graph.

3.2. HOG features based recognition

The evaluation of the performance of HOG based method is similar to the Vein based approach. Table 4 shows some of the evaluation results of HOG based identification approaches. It is observed that the system produced **89.86%** the highest GAR rate with the minimum ERR of 10.13 where FAR and FRR was 17.33, 2.93 respectively. Fig. 5 depicts the intersection point and the relation between FAR and FRR. Fig. 6 depicts the ROC curve of FAR against the GAR respect to the accuracy of the system.

Table 4. Performance of the system based on **HOG Features** method on optimal threshold values.

	Threshold	FAR (%)	FRR (%)	EER (%)	GAR (%)
	0.1	3.467918	92.33333	47.90063	52.09937
	0.35	12.13771	11.2	11.66886	88.33114
HOG features	0.2	6.935835	52.8	29.86792	70.13208

Threshold	FAR (%)	FRR (%)	EER (%)	GAR (%)
0.3	10.40375	19.33333	14.86854	85.13146
0.4	13.87167	6.533333	10.2025	89.7975
0.5	**17.33959**	**2.933333**	**10.13646**	**89.86354**

3.3. Geometric features based recognition

The evaluation of the performance of system using Geometric features also similar to the Vein based method. The efficient identification was achieved with the 94.39 rate of GAR. Where the FAR and FRR generated the score of 5.61, 5.6 respectively. The minimum EER was achieved with 5.60%. Table 5 shows some of the system performances while minimum ERR was achieved in between threshold value 0.1 to 0.5. Fig. 5 depicts the relation between FAR and FRR. Whereas Fig. 6 depicts system accuracy using ROC curve of the FAR against the GAR.

Table 5. Performance of the system based on **Geometric Features** method on optimal threshold values.

	Threshold	FAR (%)	FRR (%)	EER (%)	GAR (%)
	0.1	0.920803	84.2	42.5604	57.4396
	0.61	**5.616899**	**5.6**	**5.60845**	**94.39155**
Geometric features	0.2	1.841606	60.66667	31.25414	68.74586
	0.3	2.762409	41.46667	22.11454	77.88546
	0.4	3.683212	26.6	15.14161	84.85839
	0.5	4.604016	15.4	10.00201	89.99799

3.4. Spectral signature features based recognition

The system performance evaluation using spectral signature features is similar to the previously discussed techniques. The system achieved maximum accuracy with the 93.51% GAR rate when the threshold was 0.07. Where FAR and FRR was 6.89, 6.06 respectively. The system is able to produce 6.48 ERR by using threshold value 0.07. Table 6 shows some of the system performances where the minimum EER was achieved when threshold value is in between 0.01 to 0.5. Fig. 5 depicts the relation between FAR and FRR and intersection point of ERR line. Fig. 6 depicts the ROC curve when the maximum GAR was achieved with respect to the system performance.

Table 6. Performance of the system based on **Spectral Features** method on optimal threshold values.

	Threshold	FAR (%)	FRR (%)	EER (%)	GAR (%)
	0.01	0.985622	46.33333	23.65948	76.34052
	0.07	**6.899356**	**6.066667**	**6.483011**	**93.51699**
Spectral Sign. Features	0.1	9.856223	3.8	6.828111	93.17189
	0.2	19.71245	1.733333	10.72289	89.27711
	0.3	29.56867	0.333333	14.951	85.049
	0.4	39.42489	0.066667	19.74578	80.25422
	0.5	49.28111	0	24.64056	75.35944

3.5. Feature fusion based recognition

All the features extracted from Vein, Geometric, HOG and Spectral signatures have been fused together by concatenation. The fused feature vectors further normalized to reduce the variance between various feature sets clubbed together. The normalized features used to perform experiment. The evaluation of performance of the system was carried out by the similar manner previously discussed sections. The system was produced the maximum GAR rate with accuracy of 98.03% when threshold value was 0.02. Whereas the minimum EER 1.96 achieved on the intersection of FAR and FRR with 2.93 and 1 respectively. The Table 7 shows some of the system performances. Fig. 5 shows the relation between FAR and FRR and Fig. 6 shows the ROC curve of system accuracy with respect to FAR and GAR.

Table 7. Performance of the system based on **Feature fusion** method on optimal threshold values.

	Threshold	FAR (%)	FRR (%)	EER (%)	GAR (%)
	0.01	1.485095	11.46667	6.475881	93.52412
	0.02	**2.931315**	**1**	**1.965657**	**98.03434**
Feature fusion	0.1	14.50108	0	7.250538	92.74946
	0.2	28.96328	0	14.48164	85.51836
	0.3	43.42548	0	21.71274	78.28726
	0.4	57.88768	0	28.94384	71.05616
	0.5	72.34989	0	36.17494	63.82506

Finally, the comparison of the performance of system using various features summarized in Table 8.

Table 8. Summary of system performance with highest accuracy (%).

	Threshold	FAR (%)	FRR (%)	EER (%)	GAR (%)
Vein features	0.13	20.30264	22.66667	21.48465	78.51535
HOG features	0.35	12.13771	11.2	11.66886	88.33114
Geometric features	0.61	5.616899	5.6	5.60845	94.39155
Spectral Sign. Features	0.07	6.899356	6.066667	6.483011	93.51699
Feature fusion	0.02	2.931315	1	1.965657	98.03434

4. Conclusion

The multimodal plant identification system is designed in this research work. The proposed approaches have been implemented on *VISLeaf* dataset. The dataset is divided into 70:30 ratio for training and testing purpose, respectively. We have adopted feature level fusion to achieve multimodal plant identification. Firstly we produced results using non-imaging spectral signatures reflectance as a features. We acquired 420*500 and 180*500 dimensions feature matrix from spectral reflectance as a training and testing set respectively. Similarly we extend the features using scanned leaf images, we produce vein features, geometric features and HOG descriptor features succeeded by fusion of these features using concatenation method and we fabricated 420*620, 180*620 dimension feature matrix as a training set and testing set respectively. The evaluation of the system performed on the various type of feature sets shows that the Vein features were able to produce maximum accuracy of 78.51% GAR with 20.30 of FAR and 22.66 FRR when threshold value was 0.13. Similarly the HOG features achieved 88.33% GAR accuracy with 12.13 of FAR and 11.2 of FRR with 0.35 threshold value. The Geometric features produced the 94.39% of accuracy with 5.16 of FAR and 5.6 of FRR with threshold value was set to be 5.60. It is observed that he spectral features were better than of Vein features and HOG features with accuracy of 93.51% of GAR with 6.48 ERR. And the FAR and FRR was 6.89 and 6.06 respectively. The system achieved highest accuracy using feature level fusion with 98.03% GAR with 1.96 ERR and 2.93, 1 FAR and FRR respectively. Feature fusion is outperformed over non-imaging spectral data only. The fusion of feature improves the GAR with 3.64%, 4.51% with respect to separate geometric features and spectral features respectively.

Acknowledgment

Recommended articles

References

Ali et al., 2017   Mouad M.H. Ali, Pravin L. Yannawar, A.T. Gaikwad

Multi-Algorithm of Palmprint Recognition System Based on Fusion of Local Binary Pattern and Two-Dimensional Locality Preserving Projection

Procedia Comput. Sci., 115 (2017), pp. 482-492

View PDF   View article   View in Scopus ↗   Google Scholar ↗

Cope et al., 2010   Cope, James S., Paolo Remagnino, Sarah Barman, Paul Wilkin, 2010. The extraction of venation from leaf images by evolved vein classifiers and ant colony algorithms. In: International Conference on Advanced Concepts for Intelligent Vision Systems, pp. 135–144. Springer Berlin Heidelberg, 2010.

Google Scholar ↗

Dalal and Triggs, 2005   Dalal, N., Triggs, B., 2005. Histograms of Oriented Gradients for Human Detection. In: 2005 CVPR, San Diego, CA, pp. 886–893, 2005.

Google Scholar ↗

Fu and Chi, 2006   H. Fu, Z. Chi

Combined thresholding and neural network approach for vein pattern extraction from leaf images

IEE Proceedings-Vision, Image and Signal Processing, 153 (6) (2006), pp. 881-892

CrossRef ↗   View in Scopus ↗   Google Scholar ↗

Green et al., 2014   Walton A. Green, Stefan A. Little, Charles A. Price, Scott L. Wing, Selena Y. Smith, Benjamin Kotrc, Gabriela Doria

Reading the leaves: a comparison of leaf rank and automated areole measurement for quantifying aspects of leaf venation

Appl. Plant Sci., 2 (8) (2014), p. 1400006

View in Scopus ↗   Google Scholar ↗

Jamil et al., 2015   Nursuriati Jamil, Nuril Aslina Che Hussin, Sharifalillah Nordin, Khalil Awang

Automatic Plant Identification: Is Shape the Key Feature?

Procedia Comput. Sci., 76 (2015), pp. 436-442

View PDF   View article   View in Scopus ↗   Google Scholar ↗

Kirchgeßner et al., 2002   Kirchgeßner, Norbert, Hanno, Scharr, Uli Schurr, 2002. Robust vein extraction on plant leaf images. In: 2nd IASTED international conference visualisation, imaging and image processing.

Google Scholar ↗

Larese Mónic, 2014 Larese, Rafael Namías, Roque M. Craviotto, Miriam R. Arango, Carina Gallo, Pablo M. Granitto

Automatic classification of legumes using leaf vein image features

Pattern Recogn., 47 (1) (2014), pp. 158-168

[📄] View PDF   View article   View in Scopus ↗   Google Scholar ↗

Mounsef and Karam, 2011   Mounsef, Jinane, Lina Karam, 2011. Automated analysis of leaf venation patterns. In: Computational Intelligence for Visual Intelligence (CIVI), 2011 IEEE Workshop on, pp. 1–5. IEEE, 2011.

Google Scholar ↗

Park et al., 2008   JinKyu Park, EenJun Hwang, Yunyoung Nam

Utilizing venation features for efficient leaf image retrieval

J. Syst. Softw., 81 (1) (2008), pp. 71-82

[📄] View PDF   View article   View in Scopus ↗   Google Scholar ↗

Price et al., 2011   Charles A. Price, Olga Symonova, Yuriy Mileyko, Troy Hilley, Joshua S. Weitz

Leaf extraction and analysis framework graphical user interface: segmenting and analyzing the structure of leaf veins and areoles

Plant Physiol., 155 (1) (2011), pp. 236-245

CrossRef ↗   View in Scopus ↗   Google Scholar ↗

Rolland-Lagan et al., 2009   Anne-Gaëlle Rolland-Lagan, Mira Amin, Malgosia Pakulska

Quantifying leaf venation patterns: two-dimensional maps

Plant J., 57 (1) (2009), pp. 195-205

View in Scopus ↗   Google Scholar ↗

Salve et al., 2016   Pradip Salve, Milind Sardesai, Ramesh Manza, Pravin Yannawar

Identification of the Plants Based on Leaf Shape Descriptors, Springer, India (2016), pp. 85-101

CrossRef ↗   View in Scopus ↗   Google Scholar ↗

Sekulska-Nalewajko et al., 2010   Joanna Sekulska-Nalewajko, J. Gocławski, Ewa Gajewska, Marzena Wielanek

An algorithm to extract first and second order venation of apple-tree leaves stained for H2O2 detection. Automatyka/Akademia Górniczo-Hutnicza im

Stanisława Staszica w Krakowie, 14 (2010), pp. 359-372

Google Scholar ↗

Shejwal, 2015   S. Shejwal, *et al.*

Automatic Plant Leaf Classification on Mobile Field Guide

Int. J. Comput. Sci. Technol. (2015), pp. 93-97

Google Scholar ↗

Siravenha and Carvalho, 2016   Siravenha, A.C., Carvalho, S.R., 2016. Plant Classification from Leaf
        Textures. In: 2016 International Conference on Digital Image Computing: Techniques and
        Applications (DICTA), Gold Coast, QLD, 2016, pp. 1–8. doi: 10.1109/DICTA.2016.7797073

        Google Scholar ↗

Tang et al., 2009   Tang, Xiaodong, Manhua Liu, Hui Zhao, Wei Tao, 2009. Leaf extraction from
        complicated background. In: Image and Signal Processing, 2009. CISP09. 2nd International
        Congress on, pp. 1–5. IEEE, 2009.

        Google Scholar ↗

Varpe et al., 2015   Varpe, A.B., Rajendra, Y.D., Vibhute, A.D., Gaikwad, S.V., Kale, K.V., 2015.
        Identification of plant species using non-imaging hyperspectral data. In: 2015 International
        Conference on Man and Machine Interfacing (MAMI), Bhubaneswar, 2015, pp. 1–4.

        Google Scholar ↗

Wang et al., 2014   Yachao Wang, Gang Wu, Lixia Ding

        Plant Species Identification Based on Independent Component Analysis for
        Hyperspectral Data

        J. Software, 9 (2014), 10.4304/jsw.9.6.1532-1537 ↗

        Google Scholar ↗

Wu et al., 2007   Stephen Gang Wu, Forrest Sheng Bao, Eric You Xu, Yu Xuan Wang, Yi Fan Chang, Qiao
        Liang Xiang, 2007. A Leaf Recognition Algorithm for Plant classification Using Probabilistic
        Neural Network. In: IEEE 7th International Symposium on Signal Processing and Information
        Technology, 2007, Cairo, Egypt.

        Google Scholar ↗

Xiao et al., 2010   Xue-Yang Xiao, Hu Rongxiang, Shan-Wen Zhang, Xiao-Feng Wang, et al.

        "HOG-based approach for leaf classification." Advanced Intelligent Computing
        Theories and Applications. With Aspects of Artificial Intelligence

        Springer, Berlin, Heidelberg (2010), pp. 149-155

        CrossRef ↗   View in Scopus ↗   Google Scholar ↗

Further reading

Automatic Plant Leaf Classification on Mobile Field Guide, 2018   Automatic Plant Leaf Classification on
        Mobile Field Guide, 2018. Available from: https://www.researchgate.net/
        publication/281116309_Automatic_Plant_Leaf_Classification_on_Mobile_Field_Guide ↗ [accessed
        Mar 10 2018].

Google Scholar ↗

Cited by (18)

Multiclass skin lesion localization and classification using deep learning based features fusion and selection framework for smart healthcare
2023, Neural Networks

Show abstract ∨

A Calculation Method for the Hyperspectral Imaging of Targets Utilizing a Ray-Tracing Algorithm ↗
2024, Remote Sensing

Discriminating Spectral–Spatial Feature Extraction for Hyperspectral Image Classification: A Review ↗
2024, Sensors

MULTI-TASK LEARNING FOR MONKEYPOX SKIN LESION SEGMENTATION AND CLASSIFICATION USING CNN AND ROOTSIFT ↗
2024, Journal of Theoretical and Applied Information Technology

Leaf Recognition for Classifying Plant Species using Convolutional Neural Network ↗
2024, 2024 3rd International Conference for Innovation in Technology, INOCON 2024

Harnessing the Power of Multimodal Data: Medical Fusion and Clas-sification ↗
2024, Advances in Nonlinear Variational Inequalities

> **View all citing articles on Scopus** ↗

Peer review under responsibility of King Saud University.